Available online at www.sciencedirect.com
SCIENCE DIRECT®
C. R. Mecanique 332 (2004) 849–858
COMPTES RENDUS MECANIQUE

Application of nonlinearly demodulated acoustic signals for the measurement of the acoustical coefficient of reflection for air saturated porous materials

Mohamed Saeid [a], Bernard Castagnède [a,*], Alexei Moussatov [a,b], Vincent Tournat [a,c], Vitalyi Gusev [d]

[a] *Laboratoire d'acoustique, UMR CNRS 6613, université du Maine, avenue Olivier Messiaen, 72085 Le Mans cedex 9, France*
[b] *L.A.S.E.C., institut Meurice, 1, avenue Emile Gryzon, B1070 Bruxelles, Belgium*
[c] *Faculty of Engineering, Hokkaido University, Sapporo 060-8628, Japan*
[d] *Laboratoire de physique de l'état condensé, UMR CNRS 6087, université du Maine, avenue Olivier Messiaen, 72085 Le Mans cedex 9, France*

Received 10 February 2004; accepted after revision 4 May 2004

Available online 11 August 2004

Presented by Évariste Sanchez-Palencia

Abstract

The present Note describes work related to the measurement of the coefficient of reflection in automotive felt materials, by using a mixed ultrasonic/audio range technique. Powerful 162 kHz ultrasonic waves are amplitude modulated in the audio range. By applying appropriate procedures borrowed from underwater nonlinear ultrasonic methods (the so-called parametric antennae), one produces low frequency (i.e. in the 5–30 kHz range) acoustical waves which are generated in the pulse echo mode by short bursts. The coefficient of reflection of various felt materials are measured, and the results are compared to the standard 'fluid-equivalent' model which describes the propagation of acoustic waves in poroelastic air-saturated materials. ***To cite this article: M. Saeid et al., C. R. Mecanique 332 (2004).***

Résumé

Application des signaux acoustiques démodulés non linéairement pour la mesure du coefficient de reflexion acoustique des matériaux poreux saturés d'air. La présente Note décrit un travail relatif à la mesure du coefficient de réflexion pour des feutres de l'industrie automobile, en utilisant une technique mixte dans le domaine ultrasons/audio. Des ondes ultrasonores de puissance à 162 kHz sont modulées en amplitude dans le domaine audio. En utilisant des procédures appropriées empruntées aux méthodes de l'acoustique sous-marine non linéaire (c'est-à-dire les antennes paramétriques), des ondes acoustiques de basse fréquence (dans la bande 5–30 kHz) sont produites dans le régime d'échos impulsionnels avec des paquets d'onde courts.

* Corresponding author.
E-mail address: Bernard.Castagnede@univ-lemans.fr (B. Castagnède).

1631-0721/$ – see front matter
doi:10.1016/j.crme.2004.05.002

Le coefficient de réflexion de divers matériaux en feutre sont mesurés, et les résultats sont comparés avec le modèle standard de « fluide-équivalent » qui décrit la propagation des ondes acoustiques dans des matériaux poroélastiques saturés par l'air. ***Pour citer cet article : M. Saeid et al., C. R. Mecanique 332 (2004).***

Keywords: Acoustics; Nonlinear acoustics; Amplitude demodulation; Coefficient of reflection; Fibrous air saturated materials; Ultrasonic audio-range mixed technique; 'Equivalent-fluid' theory

Mots-clés : Acoustique ; Acoustique non linéaire ; Démodulation d'amplitude ; Coefficient de réflexion ; Matériaux poreux saturés d'air ; Technique mixte ultrasons-audio ; Théorie de fluide équivalent

Version française abrégée

Le contrôle non destructif (CND) des matériaux poroélastiques insonorisants par des techniques ultrasonores de basse fréquence (BF) est très intéressant du fait des potentialités pour effectuer des caractérisations des matériaux à distance (mesures in situ), et sur les chaînes de production (contrôle de fabrication 'on line'). Depuis une douzaine d'années, des progrès importants ont été effectués en laboratoire pour l'application des méthodes du CND par ultrasons aux matériaux poreux, à la fois pour des configurations en réflexion, en transmission ou bien avec des ondes de surface [1–3]. Ces techniques ont notamment permis de mesurer avec précision de nombreux paramètres physiques fondamentaux, pour la description de l'acoustique de ces matériaux, tels que la porosité, la tortuosité, les facteurs de forme (ou longueurs caractéristiques) associés aux pertes visqueuses et thermiques [4]. En général, ces mesures effectuées en laboratoire sont réalisées entre 20 et 60 kHz. Les mesures d'absorption (ou d'impédance de surface) sont par exemple effectuées en géométrie confinée (tube à impédance) [5].

La nouveauté dans la méthode proposée ici est d'utiliser une interaction classique de l'acoustique non linéaire d'auto-démodulation d'amplitude (ou rectification). Un transducteur ultrasonore de puissance (pompe) fonctionnant à 162 kHz envoie un signal modulé en amplitude sous la forme de paquets d'onde (tone burst), cf. Fig. 1 pour des exemples des signaux utilisés, et Fig. 2 pour le synoptique de l'expérience menée, avec des détails sur les électroniques mises en jeu. Cette technique est connue depuis 50 ans dans le domaine de l'acoustique sous-marine [6–9], et elle fut étendue par la suite en acoustique aérienne essentiellement aux U.S.A. [10–12]. Du fait de difficultés dans la mise en oeuvre pratique, notamment à cause d'une faible efficacité dans l'air, ce n'est que dernièrement que des premiers prototypes ont pu voir le jour dans le domaine de l'ingéniérie audio (du type 'audio spot-light') [13]. Les applications pour la caractérisation des matériaux granulaires ont été étudiées au Mans [14–16], et un brevet a été déposé en 2003 [17] pour des applications sensibles dans le domaine des études portant sur les matériaux poroélastiques. Nous présentons dans ce travail des données relatives au coefficient de réflexion avec ces techniques, sachant que notre équipe a déjà travaillé sur le sujet par le passé avec des méthodes classiques de l'acoustique ultrasonore [18–21]. D'autres travaux en cours [22] seront présentés ailleurs.

Les résultats essentiels de cette étude sont reportés sur les graphes de la Fig. 3 qui montrent le coefficient de réflexion pour 3 plaques de matériau poreux (feutres thermiques de l'industrie automobile). Des oscillations de ce coefficient en fonction de la fréquence sont observées d'autant plus nombreuses que l'épaisseur h de la plaque poreuse est grande. Ces fluctuations correspondent à des interférences (constructives ou destructives) partielles se produisant à l'intérieur de la plaque de matériau poroélastique. Un modèle élémentaire (non détaillé dans cette note) permet d'aboutir à l'Éq. (1) du coefficient de réflexion. C'est cette quantité qui est comparée sur la Fig. 3 aux valeurs expérimentales, les oscillations (interférences) étant dues aux termes en cosinus et en sinus de l'Éq. (1). Le vecteur d'onde k_{mat} au sein du matériau est lui-même fourni par les équations suivantes du texte qui ont permis de calculer à la fois $R(\omega)$ de la Fig. 4, et la courbe de dispersion $c(\omega)$ de la Fig. 5. Les résultats sans être excellents sont tout à fait corrects comme l'atteste la discussion menée autour du Tableau 1. On compare ici les valeurs expérimentales de l'écart de fréquence Δf des différentes résonances (ou antirésonances) pour chaque plaque poreuse (d'épaisseur 5, 10 et 20 mm), dans le cadre de plusieurs approximations. Tout d'abord, on effectue un

calcul des écarts de résonance en prenant une vitesse de propagation dans le matériau égale à celle du son dans l'air libre ($c_0 = 340$ m/s, cf. colonne (b)). Ensuite, on calcule ces écarts en utilisant la correction à fréquence infinie due à la tortuosité à l'aide de la relation $c_\infty = (1/\sqrt{\alpha_\infty})c_0$. Enfin, on procède à une correction plus fine en prenant en compte la valeur de vitesse de propagation acoustique à une fréquence donnée, obtenue directement sur la courbe de dispersion de la Fig. 5. Ce n'est que dans ce dernier cas que l'écart de fréquence Δf se rapproche des valeurs expérimentales indiquées dans la deuxième colonne du Tableau 1.

Les résultats présentés dans cette note sont remarquables, car ils constituent les premières mesures fines directes du coefficient de réflexion sur la bande 4 à 40 kHz couvrant une large partie du registre audio, ainsi que le domaine des ultrasons BF. La démodulation paramétrique permettrait en partant d'une pompe ultrasonore de plus basse fréquence (par exemple 40 kHz) d'effectuer ces mesures sur une bande plus basse, de l'ordre de 0,5 à 10 kHz tout à fait centrées dans le domaine audio. Il faut remarquer que de très nombreuses autres mesures sont dorénavant possibles avec cette technologie des ultrasons démodulés aussi bien en rétrodiffusion qu'en transmission, permettant par exemple d'obtenir la porosité, la tortuosité, les longueurs caractéristiques, le coefficient d'absorption [22]. De plus, des applications potentielles industrielles importantes concernent les mesures in-situ et les mesures 'on-line' pouvant être effectuées directement sur les sites de production des matériaux insonorisants.

1. Position of the problem

The Quantitative Non Destructive Evaluation (QNDE) of air-saturated poroelastic materials with low frequency (LF) ultrasonic techniques is quite interesting both for laboratory control purposes as well as for the potential applications to remote characterization in-situ measurements, and for the 'on-line' monitoring of production of industrial porous materials (such as fibrous felts and plastic foams). During the last 15 years, significant progress has been achieved in the field of QNDE laboratory measurements, including reflection and transmission configurations, and using in some cases surface waves above poroelastic layers [1–3]. These numerous ultrasonic techniques allow us to determine, with high accuracy, fundamental physical parameters which are crucial for the theoretical description of the propagation of acoustic waves in porous media, e.g. porosity, tortuosity and the shape factors related to the viscous and thermal dissipative exchanges within the porous medium [4]. Usually, these laboratory measurements are performed between 20 and 60 kHz. At higher frequencies (>100 kHz), some limitations exist due to the material absorption which becomes drastic, and because the mechanism of scattering (Rayleigh-like, and then multiple scattering) is more and more present as the wavelength decreases and compares to the dimensions of the pores (dimensions or distances between fibres, cells and grains).

Air-saturated porous materials are used for their absorbing properties in the audio range. Absorption (or surface impedance) measurements are often done in confined geometry by using an impedance (or Kundt) tube [5]. The very same measurements can also been achieved in the free field, but in such case one should be very careful with anechoicity in order to avoid superimposing ancillary reflections on the room walls and ceiling. Most often these measurements should be done in anechoic chambers and/or by implementing adequate temporal windowing techniques in order to avoid spurious reflections and unwanted acoustic events.

In order to by-pass some of the above limitations, a mixed ultrasonic/audio range free field technique is proposed. It is based on a nonlinear amplitude demodulation phenomenon occurring in a very strong pump ultrasonic wave during its propagation in air (or inside the porous medium). One starts with an intense beam of ultrasound wave, here with a transducer working in the tone-burst regime around 162 kHz. This powerful ultrasound wave is electronically amplitude modulated at a frequency in the range between a few kHz and 30 kHz, enabling to cover most of the audio range, and the beginning of the ultrasonic region. Fig. 1(a)–(d) provides a few examples of electric as well as acoustical temporal signals, and their corresponding power spectrum. Due to a spatial cumulative process and to the nonlinearity of air, some demodulation (or rectification) of the transmitted acoustical waves occurs over a given distance, called the aperture of the parametric array. The phenomenon was first discovered 50

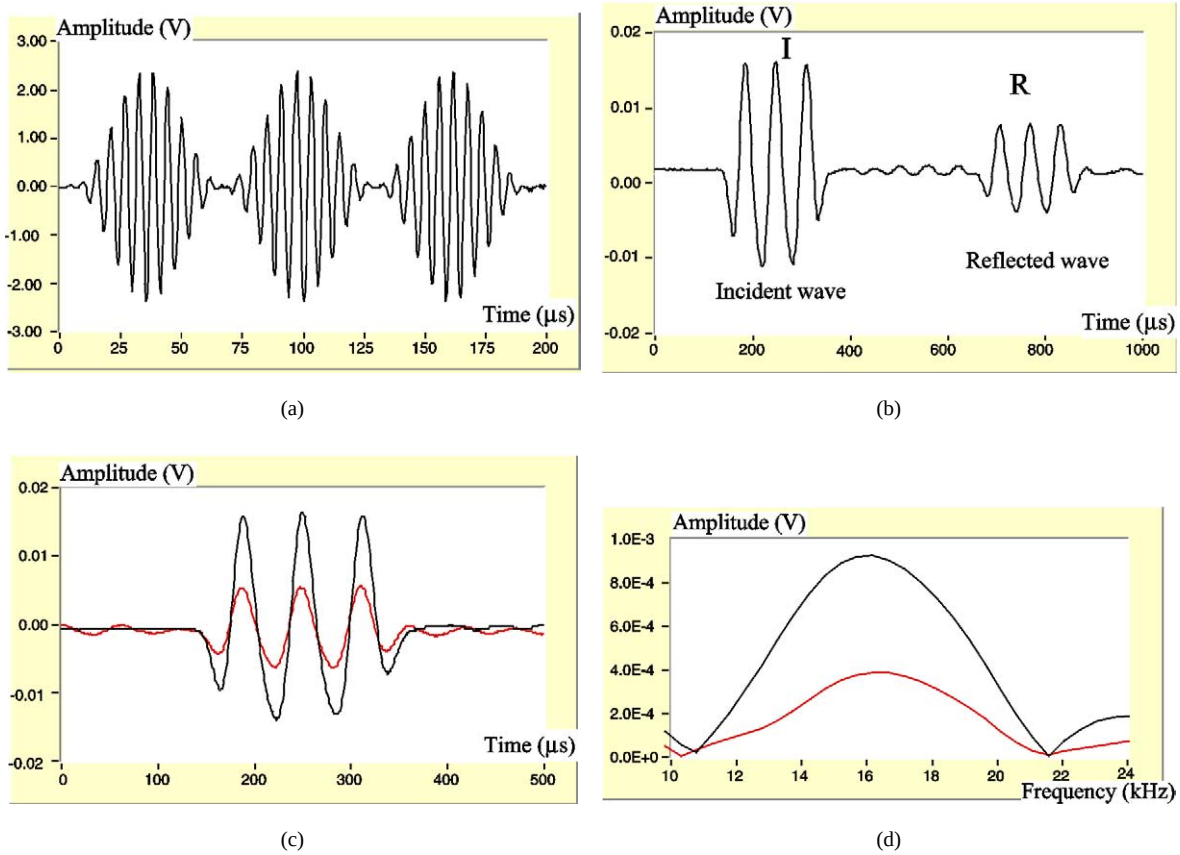

Fig. 1. Examples of some signals and their corresponding power spectrum. (a) Electric signal feeding the pump ultrasonic transducer. The carrier frequency is 162 kHz, while the modulation frequency is 16 kHz. There are three such burst composing the wave-packet; (b) Acoustic signal corresponding to (a) after propagation in 60 cm of free air, and partial reflection onto the surface of the porous material (the acquired signal is averaged 1000 times); (c) The same signal as in (b) after numerical treatment on the computer in order to superimpose temporally the incident and reflected signal; (d) The power spectrum corresponding to each wave-packet of (c).

Fig. 1. Exemples de quelques signaux et de leurs spectres respectifs. (a) Signal électrique alimentant le transducteur ultrasonore de pompe. La fréquence de l'onde porteuse est 170 kHz, alors que celle de la modulation est fixée à 16 kHz. Il y a trois éléments de ce type qui constituent le paquet d'onde ; (b) Signal acoustique correspondant à (a) après propagation dans 60 cm d'air libre, et réflexion partielle sur la surface du matériau poreux (le signal enregistré est moyenné 1000 fois) ; (c) le même signal que en (b) après traitement numérique sur ordinateur en vue de superposer temporellement les signaux incident et réfléchi ; (d) le spectre de puissance correspondant à chaque paquet d'onde de (c).

years ago in the field of underwater acoustics by Russian researchers [6–9]. It was extended afterwards in the 1980s to sound waves in air, mainly by American researchers [10–12].

Due to some difficulties in building efficient parametric arrays in air, applications were postponed until very recently, starting a few years ago with practical implementations in audio-engineering [13], such as the so-called audio 'spot-light'. These systems take advantage of the high directivity of parametric arrays in air which are at the order of the directivity of the high frequency pump wave, and even in some cases better. In fact, the directivity pattern, is theoretically provided by the length of the parametric array (or antenna) which is given by the diffraction length in air for the high frequency. For instance, in the case of the present study, with 162 kHz, this diffraction length approximately extends over 0.5 m. Beyond that distance, the pump wave is already sufficiently damped out, for the nonlinear rectification interaction not to take place furthermore. In other words, the demodulation process is efficiently achieved over a finite distance from the pump transducer, and beyond that distance (the so-called

parametric antenna dimension), no further nonlinear demodulation will occur, and only propagation in the linear regime will take place.

Further applications of parametric array in material science was done recently in granular media [14–16]. In 2003, a French patent was also submitted to INPI [17], in view of the numerous potential applications in the field of QNDE of porous media with these techniques. The present work reports on preliminary measurements achieved with a parametric array in the reflection configuration on automotive felts. The same team made during the last years various work dealing with the coefficient of reflection studied by classical ultrasonic techniques [18–21]. The novelty of the research presented below is lying on the use of this non linear rectification process. Other efforts in the course of a Ph.D. thesis will be reported elsewhere [22].

2. Experimental procedures and results

The experimental set-up which has been used is described on Fig. 2. As explained above, one uses a powerful carrier (or pump wave) at 162 kHz, for instance amplitude modulated at 16 kHz. These numbers make in turn that there are ten pseudo-periods of the carrier wave in each single modulated burst, as shown in Fig. 1(a), on the electric signal which feeds the ultrasonic transducer. The distance d_1 between the transducer and the microphone is around 60 cm, while d_2 lies near 8 to 10 cm. Accordingly, as shown on Fig. 1(b), the incident and the reflected signal at the surface of the material are temporally separated, because the wavelength at the modulation frequency (16 kHz in this case) is close to 20 mm. The experimental configuration is specifically designed to forbid constructive and

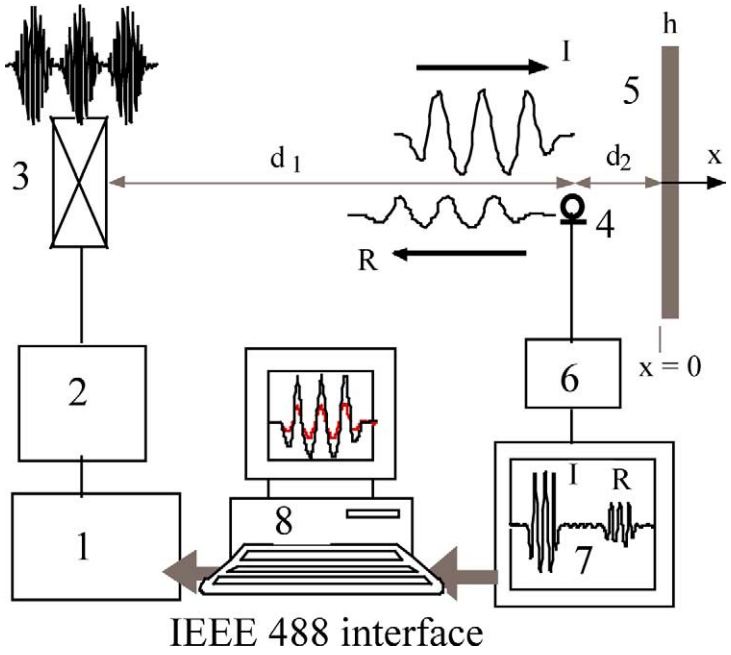

Fig. 2. Schematic for the experimental set-up. 1: Agilent HP 33120A wave generator. 2: Bruel & Kjaër 2713 power amplifier. 3: Parsonics narrow band transducers 162 kHz central frequency. 4: BK half inch microphone. 5: Porous material (FT2000 automotive felt). 6: BK microphone amplifier. 7: LeCroy 9310A oscilloscope. 8: Apple G4 personal computer with IEEE 488 interface.

Fig. 2. Schéma de principe du banc expérimental. 1 : Générateur d'onde Agilent HP 33120A. 2 : Amplificateur de puissance Bruel & Kjaër 2713. 3 : Transducteurs à bande étroite Parsonics de fréquence centrale 162 kHz. 4 : Microphone BK demi-pouce. 5 : Matériau poreux (feutre automobile FT2000). 6 : Amplificateur de microphone BK. 7 : Oscilloscope LeCroy 9310A. 8 : Ordinateur personnel Apple G4 avec bus IEEE 488.

destructive interferences over the d_2 path distance between the microphone and the material, while it is allowed within the porous plate (as its thickness h is 5, 10 or 20 mm). In fact, 3 bursts having a 16 kHz modulation frequency, extend spatially over 60 mm, and this number is amply sufficient to achieve interferences inside the porous plate. Most of the electronic features of the instruments are shown in Fig. 2. Two Agilent HP 33120A wave generators are used in order to produce arbitrary series of tone-bursts with proper amplitude modulation. A very low noise Bruel & Kjaër 2713 power amplifier is then feeding the Parsonics narrow-band 162 kHz transducer, which is ideal to achieve very strong ultrasonics fields in air with an adequate coupling front layer. The power amplifier is used at the maximum level allowed by the transducer in the tone-burst regime, in this case + 40 dB, while the output level on the Agilent HP 33120A is put at 5 V, making in turn a 500 V amplitude of the final tone burst (which correspond approximately to a pression increase of a few 102 Pa, i.e. a relative change in pressure around 10^{-3} with respect to the static atmospheric pressure, far from being negligible). To produce and optimize the very best result an additional electronics box (not shown on Fig. 2) is used in order to adapt the electric impedance of the electric signal fed onto the power amplifier.

After propagation, the acoustical signal is received on the BK microphone, and further captured on a LeCroy oscilloscope. At that point, and because the signal to noise ratio is small, it is crucial to perform time averaging, here systematically taken 1000 times. An example of the obtained temporal signal is provided on Fig. 1(b), where the incident and reflected tone bursts (with 3 modulation periods) are clearly seen. Such temporal signal is then further processed by a computer with IEEE488 interface for acquisition purpose. The incident and reflected wave packets are separately processed in the Fourier domain, and Fig. 1 (c) and (d) show the superimposed temporal profiles, as well as their corresponding power spectrum. In order to compute the coefficient of reflection versus frequency, one then needs to perform the division of the two power spectra over their bandwidth (for instance extending from 13 to 19 kHz at −6 dB on Fig. 1(d)). Some refinements should also be included in the numerical treatment in order to avoid spurious and noisy effects in the Fourier domain. For instance, the temporal signals (they are shown with raw data on Fig. 1(c)) should first be windowed in order to eliminate the tiny oscillations at the onset of the recorded signals but also on the tail. These small oscillations are responsible of phase fluctuations which can add some numerical problems during the signal processing.

The results obtained are shown on Fig. 3 in the format of the coefficient of reflection versus frequency over the obtained bandwidth. The number of bursts in a single wave-packet could evidently be changed. In the performed work, we have used either one, two or three bursts per wave-packet (even if here only the case with 3 bursts has been documented on Fig. 1). We have verified that the results in term of the coefficient of reflection are totally reproducible when changing the number of bursts. It is very useful to decrease to one single burst per wavepacket because in that case the produced bandwidth is increased accordingly. For instance with the same signal as the one shown on Fig. 1, when one single burst is used, the bandwidth at −6 dB extends from 10 to 24 kHz. By modifying as well the modulation frequency, one can record the coefficient of reflection over separate bandwidths which superimpose their results. It has been possible to record the coefficient of reflection with the 162 kHz pump transducer over the total frequency range extending from 4 to 35 kHz. The results shown on Fig. 3 concern some thermal automotive felts for 3 different plates made of the same material, having 5, 10 and 20 mm thicknesses, which are compressed at various compression ratios. The results of the coefficient of reflection versus frequency exhibit some oscillations. These variations are explained in the next section and are due to partial interferences within the porous plates which are present because the spatial width of the transmitted wave-packet extents beyond the thickness of the plate as it was estimated above.

3. Theoretical modelling and interpretation

The incident wave arrives onto the porous plate, in $x = 0$. Part of it is transmitted inside the material having thickness h, while the remaining part is reflected back. The transmitted component is then further reflected on the

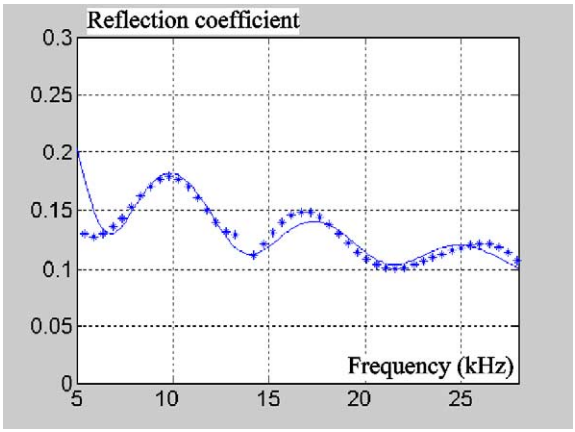

(a)

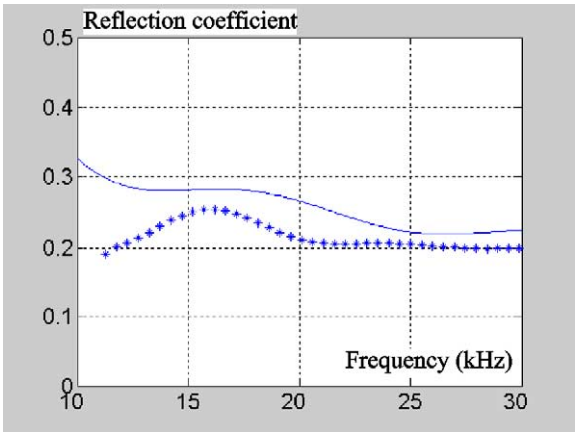

(b)

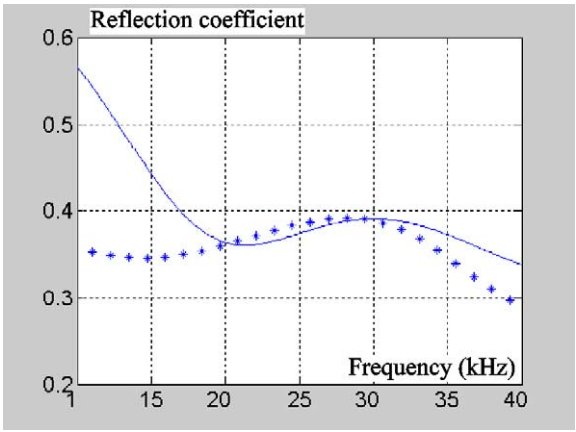

(c)

Fig. 3. Comparison of the experimental to the numerically predicted coefficient of reflection versus frequency, for three plates of FT2000 thermal felts manufactured by Rieter, having different thicknesses. (a) $h = 20$ mm, with the modulation frequency taken into steps first at 8 kHz, and secondly at 32 kHz; (b) $h = 10$ mm, with the modulation frequency taken at 22 kHz; (c) $h = 5$ mm, with the modulation frequency taken at 24 kHz. For each curve, the carrier pump wave frequency is fixed at 162 kHz.

Fig. 3. Comparaison entre le coefficient de reflexion expérimental et les prédictions numériques en fonction de la fréquence, pour trois plaques de feutres thermiques FT2000 fabriquées par Rieter, ayant différentes épaisseurs. (a) $h = 20$ mm, avec la fréquence de modulation choisie à deux valeurs, d'abord à 8 kHz, puis pour 32 kHz ; (b) $h = 10$ mm, avec la fréquence de modulation fixée à 22 kHz ; (c) $h = 5$ mm, pour la fréquence de modulation prise à 24 kHz. Pour chaque courbe, la fréquence de l'onde porteuse est fixée à 162 kHz.

second interface (at $x = +h$) while part of it is fully transmitted on the other side. Without going into details, it can be easily shown that the coefficient of reflection on the first interface can be written as [22]:

$$R(\omega) = \frac{j(\phi^2 - z_{\text{mat}}^2)\sin k_{\text{mat}}h}{2\phi z_{\text{mat}}\cos k_{\text{mat}}h + j(\phi^2 + z_{\text{mat}}^2)\sin k_{\text{mat}}h} \tag{1}$$

where $z_{\text{mat}} = \sqrt{K(\omega)\rho(\omega)/\gamma P_0\rho_0}$ denotes the acoustical impedance of the material relative to air, and k_{mat} the wavenumber. In the expression of z_{mat}, the compressibility $K(\omega)$ and the effective density of the fluid $\rho(\omega)$ are given by the following equations [4]:

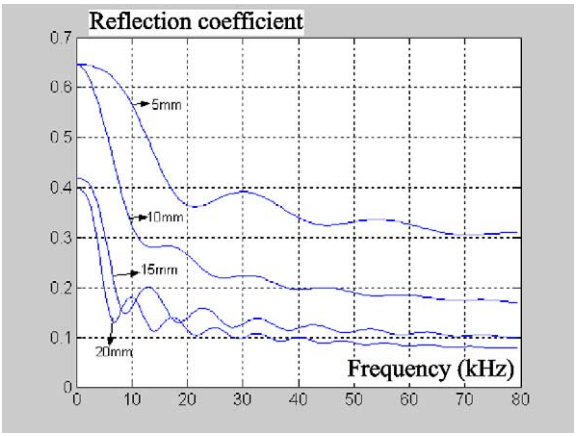

Fig. 4. Composite drawing with numerical predictions similar to those of Fig. 3 with a larger spectral extension, showing more clearly the amplitude oscillations of the coefficient of reflection, and enabling to estimate the Δf parameters of Section 2.

Fig. 4. Dessin composite obtenu avec une simulation numérique similaire à celle de la Fig. 3 avec une largeur spectrale plus grande, permettant de mieux voir les oscillations d'amplitude du coefficient de réflexion, et autorisant l'estimation du paramètre Δf de la Section 2.

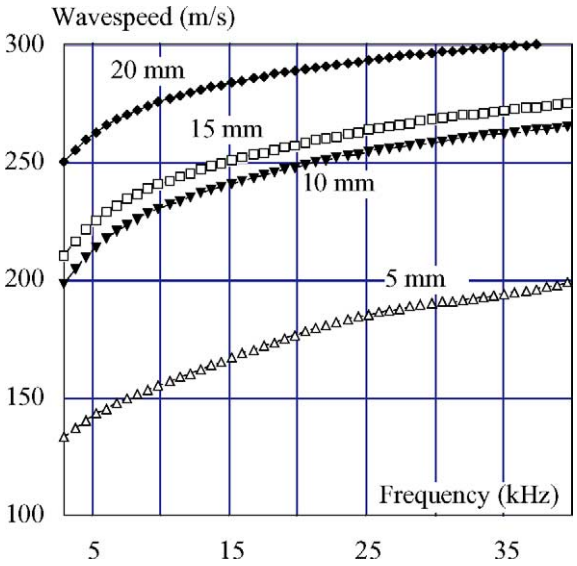

Fig. 5. Experimental dispersion curves for the very same plate as shown on Fig. 4, enabling to compute the wavespeeds versus frequency which are needed in the last columns of Table 1.

Fig. 5. Courbes de dispersion expérimentale pour exactement les mêmes plaques que celles de la Fig. 4, permettant de calculer les vitesses en fonction de la fréquence qui sont nécessaires pour les dernières colonnes du Tableau 1.

$$K(\omega) = \gamma P_0 \Big/ \left[\gamma - (\gamma-1)\left\{1 + \frac{\sigma'\phi}{j\,Pr\,\omega\rho_0\alpha_\infty} G'_J(Pr\omega)\right\}^{-1}\right]$$

$$\rho(\omega) = \alpha_\infty \rho_0 \left[1 + \frac{\sigma\phi}{j\omega\rho_0\alpha_\infty} G'_J(\omega)\right]$$

where

$$G_J(\omega) = \sqrt{1 + \frac{4j\alpha_\infty^2\eta\rho_0\omega}{\sigma^2\Lambda^2\phi^2}}, \qquad G'_J(Pr\,\omega) = \sqrt{1 + \frac{4j\alpha_\infty^2\eta\rho_0\omega\,Pr}{\sigma'^2\Lambda'^2\phi^2}} \tag{2}$$

with $\sigma' = 8\alpha_\infty\eta/(\Lambda'^2\phi)$. In these expressions, γ represents the specific heat ratio, P_0 the atmospheric pressure, Pr the Prandtl number (i.e. the ratio of the cinematic viscosity to the thermal diffusivity), ϕ the porosity, α_∞ the tortuosity, $\omega = 2\pi f$ the angular frequency, σ the air flow resistivity, ρ_0 the air density at rest, η the air viscosity, and Λ and Λ' the viscous and thermal characteristic lengths [4].

In order to derive Eq. (1), one starts by writing plane waves for the incident, reflected and transmitted waves at both interfaces. The use of plane waves is totally satisfactory with parametric nonlinear demodulation, because of the very high directivity of the transducer as it was previously discussed in Section 1. The next step is to use the Euler equation in order to calculate the particles displacement velocities. Then one needs to use the equations of continuity on the two interfaces both on acoustic pressure and on particle velocities. Accordingly, there are four equations for the four unknowns of the problem which are the amplitudes of the various acoustic fields. After some algebraic manipulations, one finally obtains the coefficient of reflection given in Eq. (1). This expression contains some trigonometric functions of $k_{\text{mat}}h$, where k_{mat} is the wave number within the material. Consequently,

Table 1
Computation of the frequency separation Δf between two consecutive resonances for the tested porous plates by considering constructive interferences with several different hypothesis. (a) Raw data taken from Fig. 4; (b) simple prediction using the speed of sound in free air; (c) prediction of the speed of sound within the porous plate in the HF asymptotic regime (including a correction term based on tortuosity); (d) from wavespeed data taken directly from the dispersion curve of Fig. 5, here at 40 kHz, which is the upper limit of the recorded spectra. This last prediction compares fairly with the experimental data

Tableau 1
Calcul du paramètre Δf écart entre deux résonances successives pour les plaques poreuses testées en prenant en compte des interférences constructives avec différentes hypothèses. (a) Données brutes prises de la Fig. 4; (b) prédiction élémentaire en utilisant la vitesse du son dans l'air libre; (c) prédiction de la vitesse du son à l'intérieur de la plaque dans le régime asymptotique HF (prenant en compte un terme de correction basé sur la tortuosité); (d) à partir de la donnée de vitesse prise directement sur la courbe de dispersion de la Fig. 5, ici à 40 kHz, ce qui correspond à la limite supérieure du spectre enregistré. Cette dernière prédiction se compare assez bien avec les données expérimentales

h (mm)	Δf_{exp} (kHz)	$\Delta f_{\text{(b)}}$ (kHz)	α_∞	Δf_8 (kHz)	$c_{40\text{ kHz}}$ (m/s)	$\Delta f_{\text{(d)}}$ (kHz)
20	7.5	8.5	1.04	8.17	300	7.35
10	14	17	1.15	16.51	265	13.80
5	24	34	1.33	30.71	205	21.35

this expression of the coefficient of reflection predicts the existence of some interferences between the incident and the reflected waves. These interferences are only partial because of the different amplitude of the sine and cosine functions. Accordingly, this result explains the oscillations of the coefficient of reflection versus frequency. The frequency spacing between two resonances (or two anti-resonances) onto the curves is simply given by $\Delta f = c_{\text{mat}}/2h$, where $c_{\text{mat}} = c(\omega) = \sqrt{K(\omega)/(\rho(\omega))}$ is the wavespeed within the porous material. Evidently, there is a drastic thickness effect, as this frequency spacing is directly related to the inverse of the thickness. One should observe much more oscillations over frequency for the thickest plate, and many fewer for the thinnest one. This is exactly what is numerically predicted and what is measured experimentally.

Additionally, one should expect a ratio between the various Δf of the different plates directly related to the change in thickness. This is not exactly the case as shown in the first columns of Table 1. With a Δf of 7.5 kHz for the thickest 20 mm plate, one should get 15 and 30 kHz respectively for the two other plates (i.e. 10 and 5 mm). There are some significant differences which are due to the fact that the wavespeed within the porous plates of various thicknesses are not the same even if the ground material is unchanged. In fact, one can compute these wavespeeds by using the high frequency asymptotic development of the 'equivalent fluid' model, that is $c_\infty = (1/\sqrt{\alpha_\infty})c_0$, where $c_0 = 340$ m/s is the wavespeed of sound waves in the free air, and where α_∞ is the tortuosity of the given porous plate. This number is calculated for each plate as well as the corresponding Δf. Unfortunately, this HF asymptotic expression for c_{mat} is valid only at very high frequencies. Here because the modulation frequency is small, in the range of 20 to 25 kHz, such expression is not valid. Instead, it is much better to directly use the numerical predictions (or alternatively the experimental measurements) of the wavespeeds for the three plates at the frequency of interest. These values drawn from the dispersion curves are used in the last column of Table 1 in order to obtain a more precise prediction of Δf for each plate. These last numbers agree quite well both with the experimental values and with the numerical predictions of Fig. 3(a)–(c) for the three thicknesses.

4. Further discussion and conclusion

The described results are important because they are the very first report on parametric demodulation of ultrasound in air with the objective to achieve very fine measurements in poroelastic materials. The covered bandwidth is very large extending from the mid-audio range around 4 or 5 kHz, up to 35 or 40 kHz. By using other frequency for the pump ultrasonic transducer, one could achieve even lower frequency measurements, down to a few 100 Hz with an appropriate low frequency pump (let us say around 40 kHz). The only limitation in such a case is the demodulation distance which will become much larger, of the order of a few meters. The achieved results

reported in the present work are of practical interest. They demonstrate that fine metrology of the coefficient of reflection is possible in porous media with parametric demodulation. This type of measurement are not possible with standard audio techniques involving simple loudspeakers and microphones, unless advanced acoustic antennae principles are used. The main advantage here deals with the simplicity of the experimental set-up which uses a single ultrasonic pump transducer, and one metrology microphone.

Other measurements have been done as well in the transmission configuration, enabling to measure tortuosity, shape factors and absorption coefficients. The transmission configuration gives also access to the measurements of the phase (or group) dispersion curves with appropriate signal processing schemes, such as phase unwrapping. These measurements are also allowed over the same bandwidth, e.g. here covering 4 to 40 kHz. These measurements will be reported elsewhere [22]. A very positive aspect of that parametric demodulation approach lies on the fact it has very large potential applications for in-situ and on-line measurements. This will provide ample opportunities for monitoring the quality of cellular and fibrous porous materials in real-time directly over the production site onto the conveyor. No other tools are presently available for that purpose.

References

[1] B. Castagnède, A. Aknine, C. Depollier, M. Melon, Ultrasonic characterization of the anisotropic behaviour of air-saturated porous materials, Ultrasonics 36 (1998) 323–341.
[2] Z.E.A. Fellah, C. Depollier, M. Fellah, Direct and inverse scattering problem in porous material having a rigid frame by fractional calculus based method, J. Sound Vib. 244 (2001) 3659–3666.
[3] L. Kelders, J.F. Allard, W. Lauriks, Surface waves above thin porous layers at ultrasonic frequencies, J. Acoust. Soc. Am. 104 (1998) 882–889.
[4] J.F. Allard, Propagation of Sound in Porous Media – Modelling Porous Sound Absorbing Materials, Chapman & Hall, London, 1993.
[5] B. Castagnède, B. Brouard, M. Henry, D. Lafarge, S. Sahraoui, Mesures des propriétés acoustiques des matériaux poreux, Techniques de l'Ingénieur R6 120 (2003) 1–24.
[6] B.K. Novikov, O.V. Rudenko, V.I. Timochenko, Nonlinear Underwater Acoustics, ASA, New York, 1987.
[7] V.A. Zverev, How the idea of a parametric acoustic array was conceived, Acoust. Phys. 45 (1999) 611–618.
[8] V.A. Zverev, Modulation technique for measuring the dispersion of ultrasound, Dokl. Akad. Nauk. SSSR 91 (1953) 791; V.A. Zverev, Sov. Phys. Acoust. 1 (1955) 353–357.
[9] H.O. Berktay, Possible exploitation of nonlinear acoustics in underwater transmitting applications, J. Sound Vib. 2 (1965) 435–461.
[10] M. Yoneyama, J. Fugimoto, Y. Kawamo, S. Sasabe, The audio spotlight: an application of nonlinear interaction of sound waves to a new type of loudspeaker design, J. Acoust. Soc. Am. 73 (1983) 1532–1536.
[11] D.T. Blackstock, Audio application of parametric array, J. Acoust. Soc. Am. 102 (1997) 3106.
[12] H.E. Bass, L.C. Sutherland, A.J. Zuckerwar, D.T. Blackstock, D.M. Hester, Atmospheric absorption of sound: further developments, J. Acoust. Soc. Am. 97 (1997) 680–683.
[13] F.J. Pompei, The audio spotlight: put sound wherever you want it, J. Audio Eng. Soc. 47 (1999) 726–731.
[14] A. Moussatov, B. Castagnède, V. Gusev, Observation of nonlinear interaction of acoustic waves in granular materials: demodulation process, Phys. Lett. A 283 (2001) 216–223.
[15] V. Tournat, B. Castagnède, V. Gusev, P. Béquin, Low frequency demodulation acoustic signatures for non linear propagation in glass beads, C. R. Mecanique 331 (2003) 119–125.
[16] V. Tournat, Effet non linéaire d'auto-démodulation d'amplitude dans les milieux granulaires : théories et expériences, Ph.D. thesis, Université du Maine, France, 2003.
[17] B. Castagnède, V. Tournat, A. Moussatov, V. Gusev, Procédé et dispositif de mesure acoustique de caractéristiques physiques de matériaux poroélastiques, brevet français déposé à l'INPI (n^{o} 0303913) le 28 mars 2003.
[18] B. Castagnède, J. Tizianel, A. Moussatov, A. Aknine, B. Brouard, Parametric study of the influence of compression on the acoustical absorption coefficient of automotive felts, C. R. Acad. Sci. Paris, Ser. II 329 (2001) 125–130.
[19] B. Castagnède, A. Moussatov, V. Tarnow, Parametric study of the influence of compression on the acoustical anisotropy of automotive felts, C. R. Acad. Sci. Paris, Ser. II 329 (2001) 295–301.
[20] M. Melon, B. Castagnède, Measurements of acoustic transmission and reflection coefficients and tortuosity of porous media at low ultrasonic frequencies, J. Acoust. Soc. Am. 98 (1995) 1228–1230.
[21] B. Castagnède, N.R. Brown, M. Melon, Mesures du coefficient de réflexion de matériaux acoustiques dans l'air à l'aide d'ultrasons basse fréquence, C. R. Acad. Sci. Paris, Ser. II 318 (1994) 1453–1457.
[22] M. Saeid, Antennes paramétriques pour l'étude de la propagation acoustique dans les matériaux poroélastiques, thèse de Ph.D. en cours, soutenance prévue en 2005, Université du Maine, France.